Brightness of Yellow Fluorescent Protein from Coral (zFP538) Depends on Aggregation†

Nadezhda N. Zubova,‡,§ Vadim A. Korolenko,‡ Artem A. Astafyev,|| Andrew N. Petrukhin,|| Leonid M. Vinokurov,⊥ Oleg M. Sarkisov,|| and Alexander P. Savitsky*,‡,§

Faculty of Chemistry, Department of Chemical Enzymology, M. V. Lomonosov Moscow State University, Vorob'ovy Gory, 119992 Moscow, Russia, Institute of Chemical Physics RAS, Kosygina str. 4, 119991 Moscow, Russia, Branch of S&O Institute of Bioorganic Chemistry RAS, Nauki Pr. 6, 142290 Pushchino, Russia, and A. N. Bach Institute of Biochemistry RAS, Leninsky Pr. 33, 119071 Moscow, Russia

Received August 11, 2004; Revised Manuscript Received December 3, 2004

ABSTRACT: The yellow fluorescent protein from coral (zFP538) forms aggregates in water solutions. According to dynamic light scattering and gel filtration data, the aggregation number is ∼1000−10000 at pH 8−9 and protein concentration 1 mg/mL. Gel filtration demonstrated that dissociation of the aggregates takes place upon dilution, and the molecular weight of the aggregates decreases with pH. Atomic force microscopy (AFM) and near-field scanning optical microscopy (NSOM) were used to obtain images of zFP538 in the solid state. It was shown that protein films are comprised of fluorescent ellipsoidal granules with a 50−300 nm major axis and a 30−130 nm minor axis. The dependence of zFP538 fluorescence on protein concentration between 1.2×10^{-9} and 5.5×10^{-7} M can be divided in two linear regions with different slopes indicating the existence of at least two different forms of zFP538. The fluorescence of zFP538 decreases with time upon acidification, and the decrease depends on pH and protein concentration. Between pH 3.5 and pH 5.5, relative residual fluorescence is higher for concentrated zFP538 solutions (about 10^{-6} M) as compared with diluted ones (10^{-7} M and below). Aggregation makes zFP538 more stable against fluorescence quenching upon acidification: the decrease in zFP538 fluorescence at protein concentration 1 mg/mL is completely reversible, unlike that observed for less concentrated solutions. This phenomenon may be due to the decrease in the freedom of chromophore mobility in zFP538 aggregates.

With the exception of green fluorescent protein (GFP)[1] from jellyfish *Aequorea victoria*, GFPs from other organisms [e.g., *Renilla reniformis*, *Renilla mullery* (the sea pansy), *Renilla kollikeri*, *Phialidium gregarium*, *and Halistaura (Mitrocoma) cellularia*] in dilute solutions form stable dimeric complexes that dissociate only under denaturing conditions (*1*, *2*). Nevertheless, the formation of dimers is best studied for GFP from *A. victoria* (*1*). GFP crystallizes as a dimer (*3*) or a monomer (*4*) depending on the conditions of crystal growth. In earlier research both hydrophobic (Ala206, Leu221, Phe223) and hydrophilic (Glu146, Asn144, Ser147, Arg168, Tyr200, etc.) amino acid residues were reported to take part in the interaction of GFP monomers to form a dimer (*3*). However, Zacharias et al. in later work (*5*) demonstrated that replacing of the hydrophobic residues at the crystallographic interface of the dimer with positively charged residues (A206K, L221K, or F223R) essentially eliminated the potential to dimerize, as was measured by analytical ultracentrifugation.

Oligomerization manifests itself in the spectral properties by the dependence of the form of the absorption spectrum on protein concentration. For *A. victoria* GFP, amplification of the main excitation peak at 395 nm at the expense of the subsidiary peak at 470 nm (*6*, *7*) is observed upon dimerization.

In the case of the coral protein, drFP583 (also known as DsRed), a great deal of experimental evidence indicates that it exists as a tetramer which is stable in solution even at low concentrations (*8*−*12*), and dimerization of tetramers with the formation of octamers occurs at higher concentration as well (*8*). However, there are no direct data on the influence of oligomerization of this protein on its spectral properties. The observed difference in peak position between a monomeric mutant and the wild-type tetramer of DsRed (*13*) may be a consequence of the intensive mutagenesis necessary to obtain monomeric DsRed, rather than to the oligomerization state. In addition to oligomerization, DsRed has a tendency to form high molecular weight aggregates. Aggregation is a common property of all novel fluorescent proteins isolated from *Anthozoa*, marine invertebrates such as corals, anemones, zoanthids, etc. (*14*). This similar aggregation behavior

† We are grateful to the Program Molecular and Cellular Biology (Russian Academy of Sciences) for financial support.

* Correspondence should be addressed to this author at the A. N. Bach Institute of Biochemistry RAS. Tel: 7(095)9548725. Fax: 7(095)-9542732. E-mail: apsavitsky@inbi.ras.ru.

‡ M. V. Lomonosov Moscow State University.

§ A. N. Bach Institute of Biochemistry RAS.

|| Institute of Chemical Physics RAS.

⊥ Branch of S&O Institute of Bioorganic Chemistry RAS.

[1] Abbreviations: AFM, atomic force microscopy; *E. coli*, *Escherichia coli*; EDTA, ethylenediaminetetraacetic acid; FPs, color fluorescent proteins; EGFP, S65T/F64L/H231L mutant of GFP; GFP, green fluorescent protein; HPLC, high-perfomance liquid chromatography; NSOM, near-field scanning optical microscopy; PBs, phycobiliproteins; SDS−PAGE, sodium dodecyl sulfate−polyacrylamide gel electrophoresis; zFP538, yellow fluorescent protein from coral *Zoanthus* sp.

10.1021/bi048274c CCC: $30.25
Published on Web 02/17/2005

can be explained by a high degree of homology between the proteins (*15*). The replacement of the positively charged residues near the N-terminus of the molecule with negatively charged or neutral residues by site-specific mutagenesis resulted in the preparation of mutant drFP583 and other fluorescent proteins from *Anthozoa* corals (zFP538, zFP506, amFP486) with reduced aggregation (*14*).

Another class of proteins that intensively absorb and brightly fluoresce in the visible region of the spectrum is phycobiliproteins (PBs), the major photosynthetic accessory proteins of cyanobacteria, red algae, and cryptomonads. Molecules of PBs contain several covalently attached linear tetrapyrrole prosthetic groups, bilins, responsible for their color. It is generally known that these proteins exhibit a strongly pronounced tendency to aggregate: phycobiliproteins can exist as monomers, dimers, trimers, hexamers, and higher molecular weight aggregates. The level of aggregation is determined by many factors, among them pH. C-Phycocyanin, for example, is a hexamer at pH 5−6 (isoelectric point of the protein), but increasing the pH to 7 results in the predominance of C-phycocyanin trimers in solution (*16*). Of course, the aggregation of PBs depends on their concentration (*17*). Aggregation is often accompanied by a hyperchromic effect and a shift both in the absorption and in the fluorescence spectra (*17*−*22*). Association of allophycocyanin monomers into a trimer is accompanied by the hyperchromic effect, a reversible 40 nm red shift in the absorption and a 22 nm red shift in the fluorescence associated with an increase in yield (*17*, *20*, *23*, *24*).

Our goal was to study fluorescence and the absorption pH profiles and the aggregation behavior of the yellow fluorescent protein zFP538 isolated from *Zoanthus* species reef corals (*15*). We have shown that pH has an influence on fluorescence and absorption of the protein. The influence is due to both the pH sensitivity of the chromophore and the pH-dependent aggregation of the protein. We used atomic force microscopy (AFM) and near-field scanning optical microscopy (NSOM) to investigate zFP538 in the solid state and kinetics measurements to study the changes of zFP538 fluorescence upon acidification.

EXPERIMENTAL PROCEDURES

Expression and Isolation of zFP538. The protein was expressed in *Escherichia coli* as a polypeptide consisting of a MRGSHHHHHHGSAQ tag at its N-terminus and amino acid sequence of the wild-type zFP538 from the 3rd to the 231st residues (*15*). *E. coli* cells were precipitated by centrifugation and destroyed by sonication in the presence of lysozyme. zFP538 was purified using a Ni-NTA column [TALON metal-affinity resin (Clontech)] according to the instructions of the manufacturer. Before elution of the protein by 1 M imidazole, the column was kept at room temperature for 24−48 h for the maturation of the zFP538 chromophore (intensive orange color was observed). zFP538 was homogeneous in the eluate according to the SDS−PAGE and HPLC data.

Spectroscopy and pH Titration. Absorption spectra were obtained on a 6405 UV−vis spectrophotometer (Jenway) and a UV-1202 UV−vis spectrophotometer (Shimadzu). pH titrations were performed on MP225 (Mettler) or PHM64 (Radiometer) pH meters with an InLab 423 microelectrode (Mettler). Fluorescence spectra were measured on a LS50B luminescence spectrometer (Perkin-Elmer). Continuous fluorescence pH profiles of zFP538 were recorded on a MPF-4 fluorescence spectrophotometer (Hitachi) with a DTS 633 automatic titration system (Radiometer), including a TTT61 digital titrator, autoburette ABU 13, and PHM64 research pH meter with continuous measurement of pH in the 1 cm path-length cell by the microelectrode.

Point-by-point measurements of fluorescence and absorption versus pH were carried out by the addition of microliter quantities of HCl or KOH/NaOH solutions to the protein sample and the subsequent measurement of fluorescence or absorption spectrum corresponding to every pH value measured by the microelectrode inside the cell.

For pH titrations the aliquots of zFP538 stock solutions were diluted into the buffers required (compositions given in the figure captions) and kept at room temperature for no less than 1 h. The zFP538 molecule contains eight Cys residues, four of which, according to the alignment with GFP (*15*), are located on the surface. β-Mercaptoethylamine was used to prevent intermolecular disulfide bond formation. The concentration of zFP538 was calculated from the optical density at 529 nm and extinction coefficient 20200 M^{-1} cm^{-1} (*15*). Absorption of the diluted zFP538 solution (5.5×10^{-7} M) was measured in a cell with 5 cm optical path length. Absorption of the concentrated zFP538 solution (5.9×10^{-5} M) was measured in a cell with 1 cm optical path length. Point-by-point measurements of fluorescence were carried out in a cell with 3 mm optical path length. Continuous measurements of fluorescence were carried out in a cell with 1 cm optical path length.

Dependence of Fluorescence Intensity of zFP538 on Protein Concentration. The dependence of fluorescence intensity on protein concentration was obtained for zFP538 solutions within the concentration range of 1.2×10^{-9}−5.5×10^{-7} M at different pH values, from pH 5 to pH 9. The stock solution of zFP538 was serially diluted 2-fold with the same buffers as used in kinetic measurements (see below), and the solutions were kept at room temperature for 1−1.5 h. The fluorescence was measured in a cell with 3 mm optical path length, 500 nm excitation, and slit widths of 15 and 20 nm. All measurements were repeated three times.

pK Determination. p*K* values were calculated from the corresponding absorption and fluorescence pH profiles by fitting the data points to a theoretical titration curve constructed for the compound with one, two, or three titrable groups (*25*). Whenever necessary, the pH profiles were segmented into several parts, and each of them was separately fitted.

Dynamic Light Scattering. Light scattering measurements for the wild-type zFP538 containing a His_6 tag were performed using a DynaPro molecular sizing instrument (Protein Solution Ltd.). Solutions of zFP538 in Tris-HCl (50 mM) and bistrispropane (50 mM) buffer, pH 9 (100 μL), were filtered through a 0.1 μm filter three times, and 12 μL aliquots were placed into a thermostatically controlled cell (at 25 °C). The final protein concentration in the cell was 4×10^{-5} M. The data were analyzed using a Dynamics V6 program that analyzes the time scale of the scattered light intensity fluctuations using a spherical model.

Gel Filtration. Gel filtration was carried out on Sephacryl S500 high-resolution (column C10/40, Pharmacia) and

Sephacryl S1000 superfine columns (column C10/20, Pharmacia); the elution rate was 0.1−0.2 mL/min. The protein was detected by fluorescence using a 420 fluorescence detector (Millipore, Waters) with a 450 nm excitation band filter and 530 nm emission cutoff filter. Calibration of the Sephacryl S1000 superfine-packed column was performed using fluorescent 120, 210, and 304 nm (5.72×10^8, 3.07×10^9, and 9.30×10^9 g/mol, respectively) Eu^{3+}-polystyrene nanoparticles (Seradyn) (338 nm excitation band filter, 530 nm emission cutoff filter) and 25 kDa chymotrypsinogen (254 nm excitation band filter, 360 nm emission band filter). The calibration curve was obtained by plotting $K_{av} = (V_e - V_0)/(V_t - V_0)$ versus the common logarithm of molecular weight (M_r) of the nanoparticles, where V_e is the elution volume, V_0 is the dead volume, and V_t is the total volume of the column (evaluated by the elution of chymotrypsinogen). The plot was linear with correlation coefficient $R^2 = 0.996$. The calibration equation was $y = -0.51x + 5.22$. The molecular mass of zFP538 was calculated for a protein concentration of 3.88×10^{-5} M at pH 8.0.

Sample Preparation for Microscopy. A small amount of the protein solution, which was preliminary dialyzed against water, was applied on a cover glass 10 or 24 mm in diameter. The sample was air-dried for a minimum of 24 h. The sample was imaged using atomic force microscopy (AFM) and near-field scanning optical microscopy (NSOM). Height and phase measurements were carried out using an AFM microscope (NT-MDT, Zelenograd, Russia) operated in the tapping mode. Height data provide three-dimensional topographical information about a sample while phase data, which measure the phase shift in cantilever oscillation, respond to attractive and repulsive interactions between the cantilever tip and a sample. This signal can be related to the stiffness of the sample. Height and near-field optical signals were measured with a NSOM head operated with shear-force feedback. A 532 nm laser emission from CW Nd:YAG was coupled to the fiber end, illuminating the sample surface through 100 nm aperture. Light transmitted through the sample was collected with a microscope objective. Transmission at each point was measured while the sample was scanned. The fluorescence spectra of the sample were measured at several points using a cooled CCD spectrometer.

Kinetic Measurements. The concentration of the stock solution of zFP538 in 2 mM EDTA (disodium salt), 0.15 M NaCl, and 2 mM β-mercaptoethylamine, pH 8.55, was 5.44×10^{-5} M, as calculated from the optical density at 529 nm and extinction coefficient 20200 M^{-1} cm^{-1} (*15*). For the kinetic measurements, 0.5, 5, or 50 μL aliquots of the zFP538 stock solution were put into a cell containing 2 mL of 50 mM EDTA (disodium salt), 0.15 M NaCl, and 2 mM β-mercaptoethylamine buffer, at pH 3.5−5.5, so the final concentration of zFP538 was 1.36×10^{-8}, 1.36×10^{-7}, and 1.33×10^{-6} M, respectively. Since the protein concentration was much less than the concentration of the buffer components, the protein was assumed to have no influence on the final pH value. The solutions were intensively stirred, and the fluorescence intensity measurements were started a maximum of 30 s after the addition of the protein into the cell. Fluorescence measurements were carried out on a LS50B luminescence spectrometer (Perkin-Elmer) in a time drive mode, at 500 nm excitation wavelength, 540 nm fluorescence wavelength, and 20 °C.

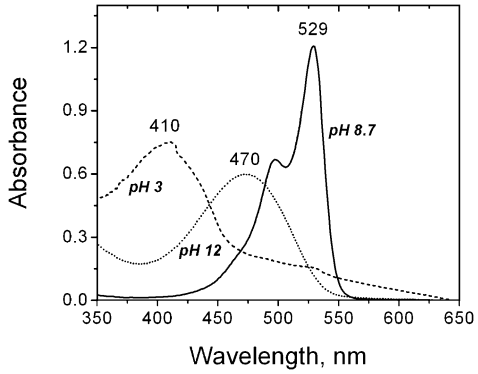

FIGURE 1: Absorption spectra of zFP538 at different pHs and buffers: 10 mM EDTA (disodium salt), 0.15 M NaCl, 0.4 mM β-mercaptoethylamine, and protein concentration 5.9×10^{-5} M.

Mathematical processing of the results was carried out using Microcal Origin 6.0.

RESULTS

Spectroscopy and pH Titration. Absorption of zFP538 was pH sensitive. The maximum at the major absorption band shifted from 529 to 410 nm upon a pH change from neutral to acidic values and to 470 nm upon a pH change from neutral to alkaline (Figure 1). zFP538 emitted yellow light with a maximum at 538−540 nm when excited at neutral pH (*15*).

At high concentrations of zFP538, $(3-5.9) \times 10^{-5}$ M, acidification resulted in a decrease in the absorption of the protein at 529 nm (Figure 2A) and a decrease in the corresponding fluorescence at 538−540 nm (Figure 3). The changes in absorbance and fluorescence were reversible at pH from 8.5 to 3.0, but fluorescence became irreversible at lower pH (pH 2.2) (data not shown). Increasing the pH to 12 gave rise to the irreversible decrease in both absorption and fluorescence (data not shown) that may be due to protein denaturation.

The absorption pH profile of the diluted zFP538 solution differed from the profile of the concentrated solution (Figure 2B). The main difference is observed in the pH range from 4 to 8: a plateau can be seen in the absorption profile of the concentrated solution whereas for the diluted one, the absorption smoothly decreases without any plateau. The profiles almost coincide at pH 3−4. It is noteworthy that the pH profiles for the reverse titration also differ. After the reverse titration of zFP538 solutions with base, the absorption was restored by only 40% for the diluted solution and was completely restored for the concentrated one.

Mathematical processing of the pH profile curves for the direct titration of zFP538 solutions resulted in the following pK values: $pK_1 = 4.3 \pm 0.1$ and $pK_2 = 6.4 \pm 0.1$ for the diluted solution and $pK_1 = 4.60 \pm 0.02$, $pK_2 = 6.13 \pm 0.08$, and $pK_3 = 7.47 \pm 0.09$ for the concentrated solution (*25*).

As the concentration of zFP538 decreases, the fluorescence pH profile shifts to the alkaline region, and at a protein concentration of $\sim 10^{-7}$ M, the additional maximum appears in the acidic region (Figure 4). Upon further decreasing the protein concentration, this additional maximum moves to the more acidic region and disappears at a zFP538 concentration of 8×10^{-9} M. pK values calculated from these profiles are summarized in Table 1. The tendency of pKs to move to the

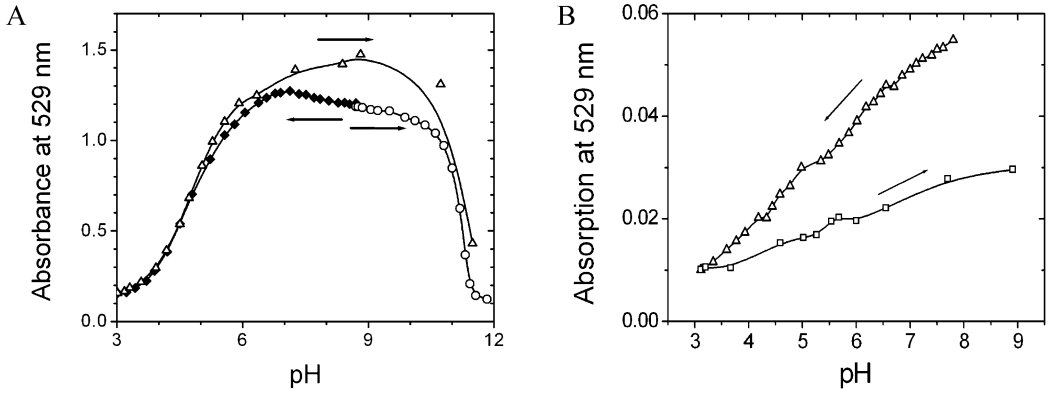

FIGURE 2: Comparison of absorption pH profiles at 529 nm for the concentrated (A) and diluted (B) solutions of zFP538. Arrows indicate directions of titration. (A) Protein concentration = 5.9×10^{-5} M. Buffers: 10 mM EDTA (disodium salt), 0.15 M NaCl, and 0.4 mM β-mercaptoethylamine. Optical path length = 1 cm. Solid diamonds show direct titration with an acid, open circles show direct titration with an alkali, and open triangles show the reverse titration from the acidic to the alkaline region. (B) Protein concentration = 5.5×10^{-7} M. Buffers: 1 mM EDTA (disodium salt), 0.15 M NaCl, and 0.4 mM β-mercaptoethylamine. Optical path length = 5 cm. Open triangles show direct titration with an acid, and open squares show reverse titration with an alkali.

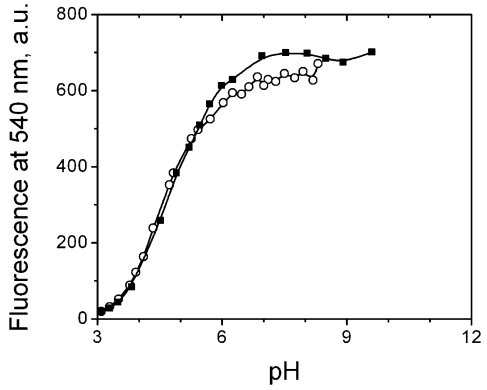

FIGURE 3: Fluorescence recovery for a concentrated zFP538 solution after acidification to pH 3. Protein concentration = 3×10^{-5} M, excitation at 520 nm, and emission at 540 nm. Buffers: 5 mM EDTA (disodium salt), 0.15 M NaCl, and 0.2 mM β-mercaptoethylamine. Open circles indicate direct titration with HCl, and squares indicate reverse titration with KOH.

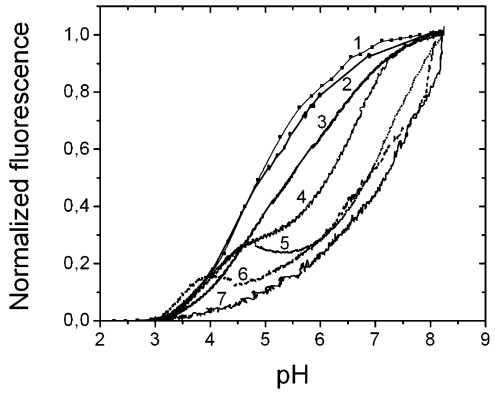

FIGURE 4: Influence of protein concentration on fluorescence pH profiles of zFP538, obtained upon direct titration by 0.1 M HCl to pH 3. Fluorescence intensities were normalized to the intensities at pH 8. Excitation was at 490−520 nm and emission at 540 nm. Protein concentration: 3.3×10^{-5} M (1), 1.7×10^{-5} M (2), 3.3×10^{-6} M (3), 5.2×10^{-7} M (4), 2.5×10^{-7} M (5), 1.3×10^{-7} M (6), and 8×10^{-9} M (7). Buffers: 5 mM glycine, citrate, phosphate (Na_2HPO_4), and 0.15 M NaCl.

more acidic and to the more alkaline values is observed as the concentration of zFP538 decreases.

Unlike the concentrated zFP538 solutions, at protein concentrations lower than 3×10^{-5} M acidification to pH 3 causes partially irreversible (at least within the experimental time) quenching of fluorescence (Figure 5). The lower the concentration of the protein, the lower the degree of recovery of fluorescence after returning to the neutral conditions. When the protein is acidified to pH ~5.2, the fluorescence of low concentration solutions (about 10^{-7} M) is fully recovered after returning to the neutral conditions (data not shown).

The fact that fluorescence pH profiles of zFP538 depend on the protein concentration indicates that oligomerization or aggregation occurs in the zFP538 solutions. At the same time these processes are shown to have no influence on the shape of the emission spectrum.

The pH-induced decrease in absorption and fluorescence for high concentration solutions of zFP538 may be explained by the alteration of the aggregation state of the protein, for example, by pH-dependent dissociation of high molecular weight protein aggregates. Similar phenomena have been observed for phycobiliproteins, whose bright fluorescence can be accounted for by the formation of large aggregates, while its dissociation into monomers commonly results in a decrease of both fluorescence and absorption (*17*, *23*).

Nonlinear Dependence of the Fluorescence Intensity of zFP538 on Protein Concentration. At all pH values from 5 to 9, the dependencies of the intensity of zFP538 fluorescence on protein concentration were nonlinear in the studied concentration range. The fluorescence−protein concentration plots can be divided into two linear portions: one with a lower slope for concentrations lower than 1×10^{-7} M and the second with a higher slope for concentrations higher than 1×10^{-7} M (Figure 6); the inflection point lies near 10^{-7} M. Thus, a transition between different aggregation states of the protein occurred at a protein concentration near 10^{-7} M. The aggregation states at lower protein concentration exhibited lower fluorescence intensity, what may have been due to either a decrease in the fluorescence quantum yield or a decrease in the extinction coefficient at the excitation wavelength. The fact that the concentrated and diluted zFP538 solutions had different absorption recovery between pH 3 and pH 8 (Figure 2) supported the latter assumption.

Aggregation Number. The calculated molecular mass based on the amino acid sequence of wild-type zFP538 for a monomer with a His_6 tag was 27.4 kDa (*15*). Dynamic light

Table 1: pK Values of zFP538 Calculated from Fluorescence pH Profiles Shown in Figure 4

concn, M	pK_1	pK_2	pK_3	pK_4	pK_5
3.3×10^{-5}		4.60 ± 0.02	6.30 ± 0.06		
1.7×10^{-5}		4.47 ± 0.01	6.17 ± 0.01		
3.3×10^{-6}		4.56 ± 0.01	6.20 ± 0.01		7.69 ± 0.01
5.2×10^{-7}	3.85 ± 0.01			6.57 ± 0.01	
2.5×10^{-7}	3.81 ± 0.01	4.68 ± 0.02		6.80 ± 0.01	7.74 ± 0.02
1.3×10^{-7}	3.41 ± 0.01[a]		5.52 ± 0.02	6.87 ± 0.01	
8×10^{-9}		4.51 ± 0.02	6.16 ± 0.02		7.89 ± 0.03

[a] Two protons are involved in the process.

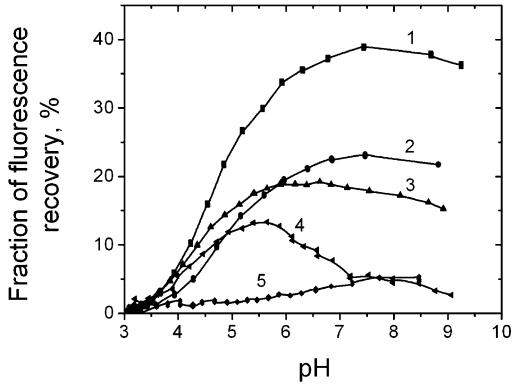

FIGURE 5: Influence of protein concentration on fluorescence recovery of zFP538 upon reverse titration from pH 3 to the alkaline region after direct titration from pH 8 to pH 3. Excitation was at 490−520 nm and emission at 540 nm. Buffers: 5 mM glycine, citrate, phosphate (Na_2HPO_4), and 0.15 M NaCl. Fluorescence intensities were normalized to the original intensity at pH 8. Protein concentration: 1.7×10^{-5} M (1), 8.3×10^{-6} M (2), 3.3×10^{-6} M (3), 1.0×10^{-6} M (4), and 8.0×10^{-9} M (5).

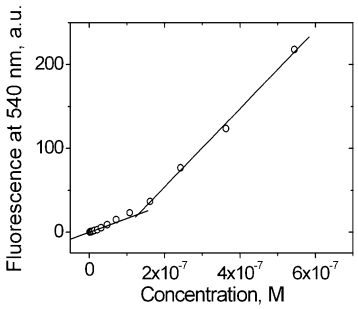

FIGURE 6: Nonlinear dependence of the fluorescence intensity of zFP538 on protein concentration at pH 7.5. The inflection point corresponds to the protein concentration 1.3×10^{-7} M.

scattering of a highly concentrated (~1 mg/mL, 4×10^{-5} M) solution of zFP538 at pH 9 showed that the protein was strongly aggregated, and the molecular mass of the protein aggregates, according to a dynamics V6 calculation using a spherical model, was 990 times higher than that of monomers.

Gel filtration experiments demonstrated that, under alkaline and neutral conditions, the dilution of zFP538 was accompanied by the dissociation of the protein aggregates (Figure 7). Moreover, according to the data obtained for low concentrations of zFP538, the molecular weight of the aggregates decreased upon changing the pH from alkaline to neutral.

On the basis of gel filtration of zFP538 on a Sephacryl S-1000 matrix, the molecular mass of the aggregates was estimated as 2.5×10^8 Da (pH 8.0, protein concentration 3.88×10^{-5} M).

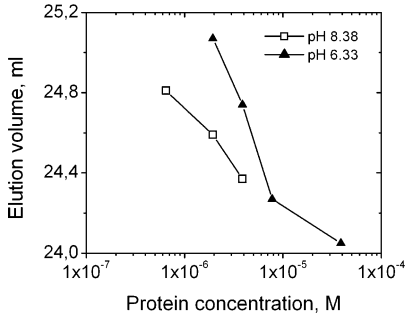

FIGURE 7: Dependence of elution volume on protein concentration upon gel filtration of zFP538 on Sephacryl S-500 at pH 8.38 (□) and pH 6.33 (▲) in semilogarithmic scale. Elution buffer: 50 mM EDTA (disodium salt), 10 mM Tris-HCl, 0.15 M NaCl, and 2 mM β-mercaptoethylamine. Elution volume increases upon decrease in protein concentration and pH.

One of the reasons for the discrepancy of the dynamic light scattering and gel filtration data may have been the fact that the real form of the protein aggregates differed from the spherical ones that were used in the model for processing the results of dynamic light scattering. However, both methods indicated the existence of high molecular weight aggregates of zFP538 with aggregation number 1000−10000.

Unlike EGFP, which crystallizes upon drying, zFP538 formed ring-like films due to its surfactant properties (Figure 8). According to AFM, these films were comprised of ellipsoidal protein granules, with the major axis of the granules lying in the range from 50 to 300 nm and the minor axis lying in the range from 30 to 130 nm (Figure 9).

As can be seen from Figure 9A,B, the granules are oriented in space in a defined manner. This orientation is, probably, radial with regard to the ring-shaped protein film. It can be hypothesized that, during the protein film formation, the molecules of the yellow protein are pulled together on the water−air interface due to surface activity. As the concentration of the protein in solution decreases, the film formed from the drops of the same volume becomes narrower and thinner but retains the ring shape.

As a control experiment, the AFM images of the cover glasses were obtained (data not shown). These data indicated that the visible surface irregularities are typical of the protein film rather than of the glass support.

zFP538 in the solid state retained its fluorescence; the emission spectrum became broader and was 12−14 nm red shifted in comparison with the spectrum of zFP538 in water solution (Figure 10). The ratio of the maximum emission to the shoulder at 580 nm is 0.65 for solid zFP538 and only 0.25 for the protein in water solution. Such a difference may result from the phenomena of internal filter and reabsorption effects in the yellow protein film.

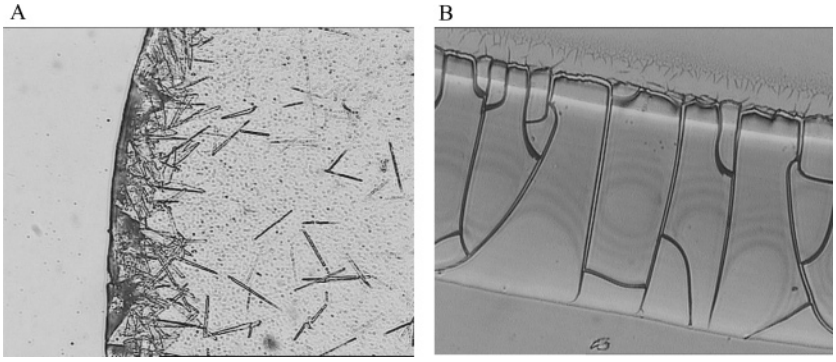

FIGURE 8: EGFP crystallizes upon drying (A) and zFP538 forms ring-like films due to its surfactant properties (B). Optical micrographs of EGFP (objective 10×) and part of the ring film of zFP538 (objective 20×) were obtained using the Olympus IX 71 microscope.

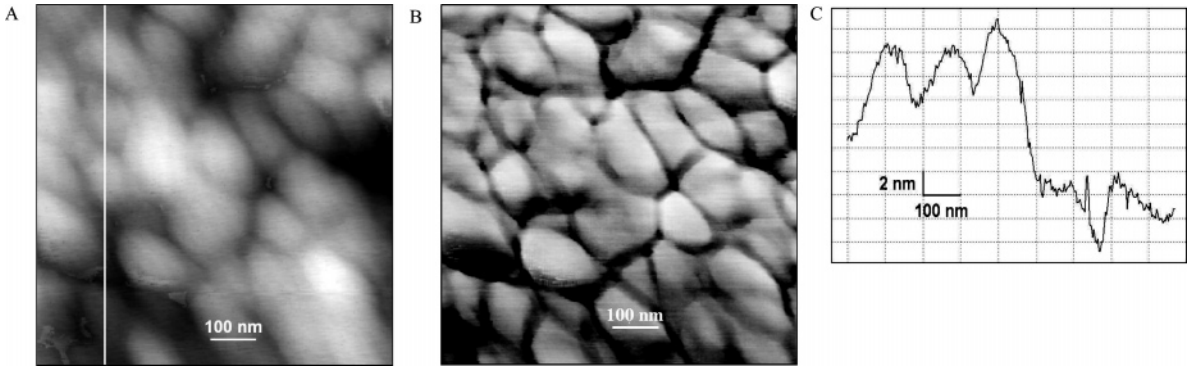

FIGURE 9: Topography (A) and phase (B) AFM images of the one and the same portion (900 nm × 900 nm) of the yellow protein film deposited on a cover glass. Lightening corresponds to the increase in height. Phase data can be related to the stiffness of the sample. (C) Section of the topography image along the white line shown in (A) gives surface geometry of the protein film.

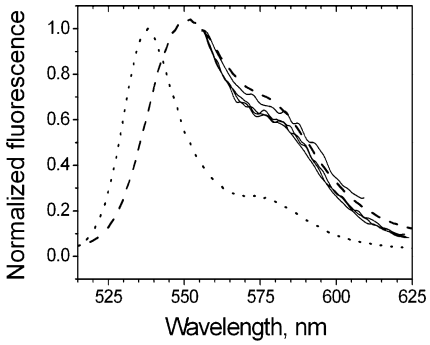

FIGURE 10: Normalized emission spectrum of a water solution of zFP538 (excitation at 480 nm, dotted line) and solid zFP538 (excitation at 480 nm, emission cutoff filter VY47 and excitation cutoff filter UV 35, dashed line), measured on a Shimadzu RF-5301PC spectrofluorophotometer; all other spectra were obtained by NSOM from different localizations of the zFP538 film (excitation at 532 nm, solid lines). The emission spectrum of the water solution of zFP538 is normalized to the maximum intensity at 540 nm, and emission spectra of solid zFP538 are normalized to the intensity at 556 nm.

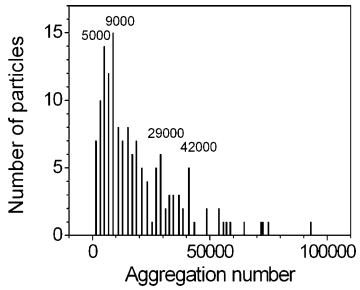

FIGURE 11: Distribution of the aggregation number of zFP538 calculated from 146 AFM images of the protein granules.

From the AFM data we calculated the volume of the granules assuming that the granules are ellipsoids of rotation. Since the three-dimensional structure of the yellow protein is still unknown, the volume of the homologous GFP molecule [cylinder 4.2 nm in height and 2.4 nm in diameter (*26*)] was taken for the monomer volume. The average volume of zFP538 granules is about 19500 times higher than the monomer volume. The distribution of the aggregation number breaks into several peaks, with aggregation numbers of 5000−9000 in the first peak and 29000 and 42000 in the minor peaks (Figure 11). Under conditions of protein film formation, about 50% of the granules belong to the fraction with the aggregation number distribution of 5000−9000, which is rather close to the aggregation number determined by gel filtration.

Kinetic Measurements of zFP538 Fluorescence upon Acidification. pH profiles of fluorescence described above correspond to the superposition of at least two processes: changes in fluorescence due to acidification and a gradual accumulation of changes in intensity due to denaturation at low pH. To elucidate the role of both of these factors, kinetic experiments at fixed pH and several concentrations were performed.

Since the dependence of intensity of zFP538 fluorescence on protein concentration is nonlinear (Figure 6), the protein concentrations corresponding to the linear portions (1.36×10^{-8} and 1.33×10^{-6} M) and to the point of the crossing of linear portions (1.36×10^{-7} M) were chosen for kinetic measurements. At pH values between 3.5 and 5.5, the fluorescence intensity of zFP538 decreased with time at all three chosen protein concentrations (Figure 12).

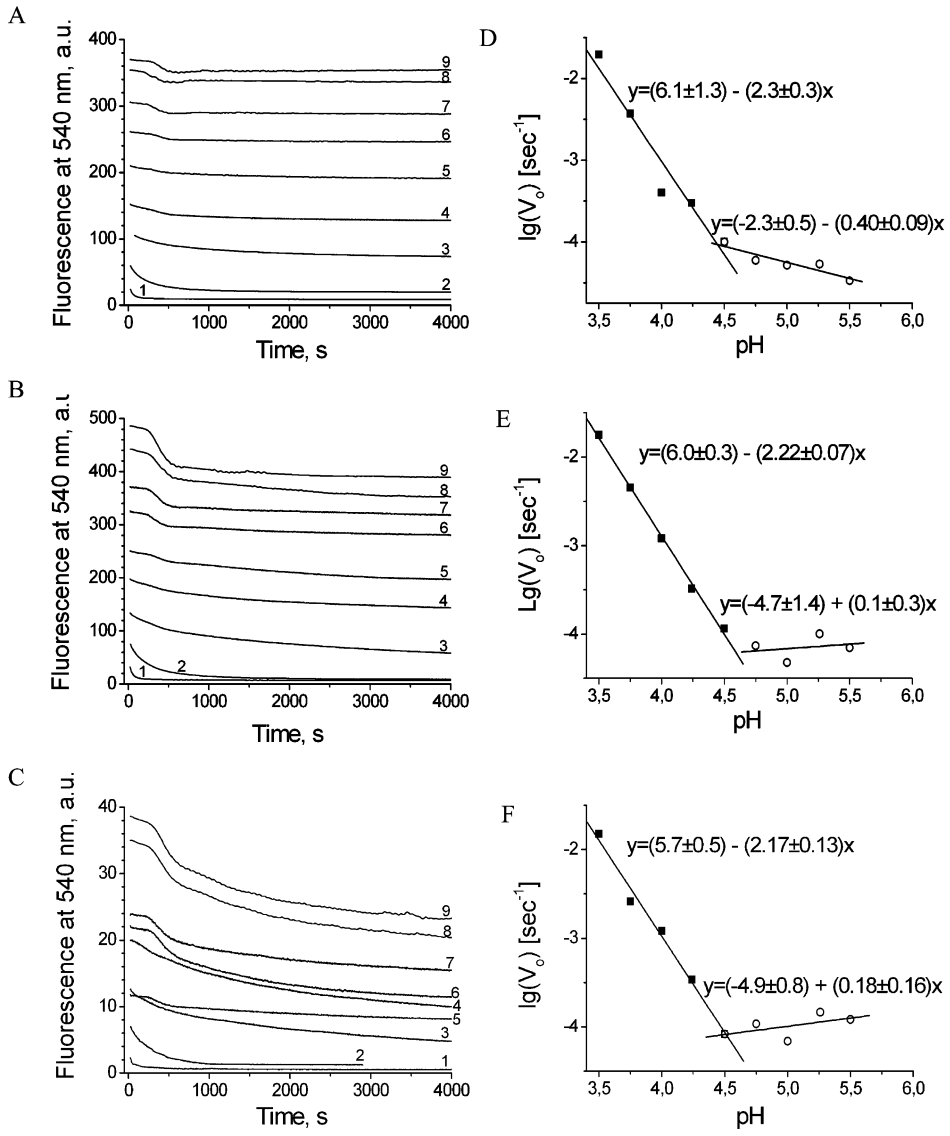

FIGURE 12: Kinetics of changing zFP538 fluorescence upon incubation at pH 3.5−5.5. The concentration of zFP538 was 1.33×10^{-6} M (A) (slit width 5 nm), 1.36×10^{-7} M (B) (slit width 15, 20 nm), and 1.36×10^{-8} M (C) (slit width 15, 20 nm). Conditions: pH 3.5 (1); pH 3.75 (2); pH 4 (3); pH 4.24 (4); pH 4.5 (5); pH 4.75 (6); pH 5 (7); pH 5.26 (8); pH 5.5 (9). pH dependencies of common logarithms of the initial rates of fluorescence decrease calculated from the slopes of the initial section of kinetic curves in panels A−C. The concentration of zFP538 was 1.33×10^{-6} M (D), 1.36×10^{-7} M (E), and 1.36×10^{-8} M (F).

For all three concentrations of zFP538, the kinetic curves at pH 3.5 were described with a three-exponential equation:

$$A = A_1 \exp(-x/t_1) + A_2 \exp(-x/t_2) + A_3 \exp(-x/t_3) + A_0 \quad (1)$$

where A is the fluorescence intensity, x is time, t_1, t_2, t_3, A_1, A_2, A_3 are characteristic time and preexponential factors, respectively, and A_0 is the residual fluorescence at infinite time.

At pH 3.75−4.24, the fluorescence intensity decreased as a double exponential relaxation:

$$A = A_1 \exp(-x/t_1) + A_2 \exp(-x/t_2) + A_0 \quad (2)$$

Further increase in pH from 4.5 to 5.5 resulted in the appearance of the plateau on the initial portion of the kinetic curves: the fluorescence decreased smoothly during the first 200−300 s and then sharply diminished according to the two-exponential law (eq 2).

Mathematical processing of the fluorescence pH profiles at infinite time (constructed on the basis of processing of the data presented in Figure 12A−C) using the modified Henderson−Hasselbalch equation (*27*)

$$\log\left(\frac{I_{max} - I_{min}}{I - I_{min}} - 1\right) = n(\mathrm{p}K) - n(\mathrm{pH}) \quad (3)$$

where n is the number of protons, K is the acid−base equilibrium constant, I_{max} and I_{min} are signals for the deprotonated and protonated forms, and I is the signal at a certain pH, gives n values of 1.30 ± 0.06, 1.30 ± 0.09, and 1.36 ± 0.17 for protein concentrations of 1.33×10^{-6}, 1.36×10^{-7}, and 1.36×10^{-8} M, respectively. Since this value differs from 1.0, the decrease in fluorescence intensity upon decrease in pH cannot be attributed to the acid−base equilibrium with participation of a single proton. The pK

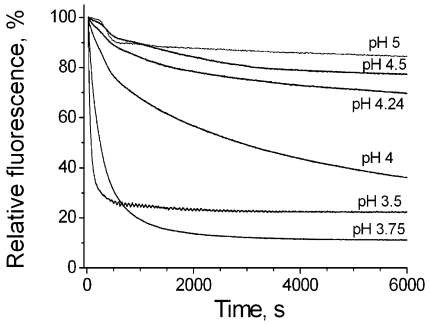

FIGURE 13: The time course of the decrease in relative fluorescence (fluorescence normalized to the initial moment of time) strongly depends on pH. The concentration of zFP538 was 1.36×10^{-7} M.

values calculated by eq 3 are 4.5, 4.5, and 4.8 for protein concentrations of 1.33×10^{-6}, 1.36×10^{-7}, and 1.36×10^{-8} M, respectively. The same p*K* values were observed for all studied fluorescence and absorption pH profiles of zFP538 (see pH titration section and Table 1).

For all zFP538 concentrations, a decrease in the relative residual fluorescence at infinite time, i.e., residual fluorescence divided by fluorescence at the initial time (A_0 parameter in eqs 1 and 2 obtained after the mathematical processing of normalized kinetic curves in Figure 13), is generally observed upon decreasing the pH. The main change occurs at pH values between 3.75 and 4.5, where A_0 decreases from ~93% to ~33% for the protein concentration 1.33×10^{-6} M, from ~80% to ~17% for the protein concentration 1.36×10^{-7} M, and from ~55% to ~17% for the protein concentration 1.36×10^{-8} M. A_0 remains practically constant at pH values between 5 and 5.5. It is important to note that the higher the protein concentration, the higher the relative residual fluorescence (A_0) over almost the entire pH range.

The analysis of the kinetics of fluorescence decrease indicates that the initial rates of the decrease depend on pH. Figure 12D−F presents pH dependencies of common logarithms of the initial rates calculated from the slopes of the initial section of kinetic curves in Figure 12A−C. These dependencies are divided into two linear portions with different slopes intersecting at pH near 4.5.

Thus, the change in the mechanism of fluorescence decrease upon decrease in pH was observed for all studied protein concentrations at pH near 4.5. It is interesting to note that the slope of linear sections at pH <4.5 is approximately the same for all protein concentrations and is equal to 2.2−2.3. This is where the difference between zFP538 and DsRed proteins can be seen since for DsRed the same dependence is linear within all pH ranges from 3.75 to 5.0 with slope equal to 4 (*28*).

The situation is somewhat different at pH > 4.5. For the solution of a protein concentration of 1.33×10^{-6} M, the initial rate is still increased upon a decrease in pH (negative value of the slope equal to -0.40 ± 0.09), but for the solutions with protein concentrations of 1.36×10^{-7} and 1.36×10^{-8} M, the initial rate is, on the contrary, decreased very weakly (positive value of the slope equal to 0.1−0.2) (Figure 12D−F). This may be explained by the appearance of the additional maximum on the continuous fluorescence pH profiles in this concentration range (about 10^{-7} M) (Figure 4) that indicates the appearance of a new spectral form, which was absent at higher zFP538 concentrations.

Spectral Changes Observed upon Acid Denaturation of zFP538. As the pH of the solution decreases, small changes in the emission spectra of zFP538 at 500−520 nm are observed after 1−2 h incubation. When passing to the acidic region, the fluorescence intensity at 508 nm increases from ~3% to ~7% (Figure 14). The change in the fluorescence emission spectrum at 560−590 nm is also observed upon incubation of zFP538 at different pH values within the studied pH range. At a protein concentration of 1.36×10^{-8} M and, to a lesser degree, at 1.36×10^{-7} M, the ratio of fluorescence intensities at 540 and 580 nm was changed upon decreasing the pH. This change is absent at high zFP538 concentration of 1.33×10^{-6} M. These changes are most noticeable at pH 3.5. As can be seen from Figure 15, during incubation at this pH, the shoulder at 580 nm increased as compared with the fluorescence intensity at 540 nm. Thus, the kinetic curves of acidic denaturation of zFP538 are complicated by the transition of one spectral form (540 nm) into another (575−580 nm) that is most noticeable at pH 3.5. This is, probably, the explanation of the appearance of the third exponent (eq 1) in the kinetic curves obtained for the incubation of zFP538 at pH 3.5.

The excitation spectra of zFP538 also changed with pH. For a protein concentration of 1.36×10^{-8} M and, to a lesser extent, 1.36×10^{-7} M and 1.33×10^{-6} M, the contribution of excitation at 390 nm increased as pH decreased. At pH 3.5, for a protein concentration of 1.36×10^{-8} M, the main peaks at 529 and 497 nm disappeared while a peak near 470 nm emerged (Figure 16).

Analysis of kinetic parameters should be carried out independently for the pH ranges 3.5−4.24 and 4.5−5.5 since the change in the form of the kinetic curves is observed at pH >4.24 (appearance of the plateau on the initial section).

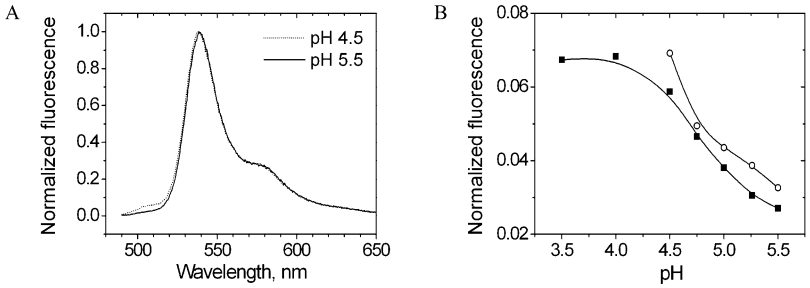

FIGURE 14: (A) Normalized to the intensity at 540 nm fluorescence emission spectra of zFP538 after 2 h incubation at pH 4.5 and 5.5. The concentration of zFP538 was 1.33×10^{-6} M. (B) Intensity of zFP538 fluorescence at 508 nm normalized to the intensity at 540 nm after 1−2 h incubation at different pHs. The concentration of zFP538 was 1.33×10^{-6} (■) and 1.36×10^{-7} M (○).

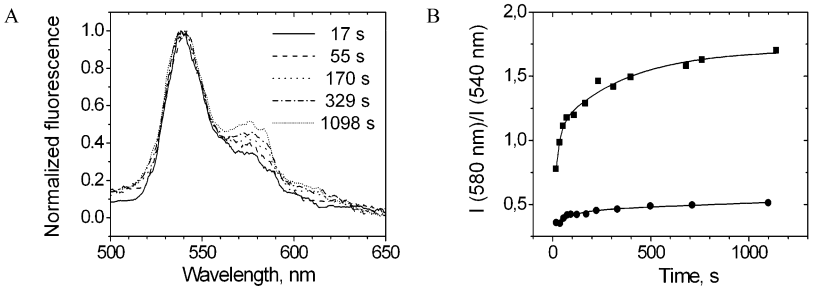

FIGURE 15: (A) Normalized to the intensity at 540 nm fluorescence emission spectra of zFP538 as a function of incubation time at pH 3.5. The concentration of zFP538 was 1.36×10^{-7} M, excitation at 480 nm. (B) Ratio of fluorescence intensities at 540 and 580 nm as a function of incubation time at pH 3.5. The concentration of zFP538 was 1.36×10^{-7} (●) and 1.36×10^{-8} M (■).

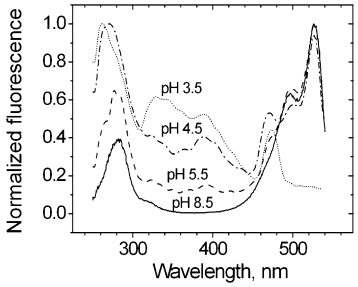

FIGURE 16: Normalized to the maximum intensity fluorescence excitation spectra of zFP538 after 1−2 h incubation at different pH. The concentration of zFP538 was 1.36×10^{-8} M; emission was registered at 560 nm.

For all protein concentrations, the "fast" rate constant decreases by approximately an order of magnitude (from 10^{-2} to 10^{-3} s^{-1}) upon changing the pH from 3.5 to 4.24. The "slow" constant varies in a similar manner (from 10^{-3} to 10^{-4} s^{-1}). At pH 4.5−5.5, the fast constant is about 10^{-3} s^{-1} and the slow one is about 10^{-4} s^{-1} for a protein concentration of 1.33×10^{-6} M. For protein concentrations of 1.36×10^{-7} and 1.36×10^{-8} M, the fast and slow constants are about 10^{-3} and 10^{-4} s^{-1}, respectively, and the fast constant at 1.36×10^{-7} M is somewhat higher than that for 1.36×10^{-8} M. At pH 3.5, the third constant (the slowest one) increases from 10^{-4} to 10^{-3} s^{-1} on the decrease of protein concentration.

DISCUSSION

Our present study allows us to conclude that, in solutions of zFP538, aggregation takes place. This aggregation depends on pH and influences the fluorescence and absorbance pH profiles and the kinetics of acidic denaturation of zFP538. The pH dependence of GFP fluorescence involves reversible and fast protonation steps at a pH >5 and both protonation and slower conformational changes at lower pH (*29*). For high concentrations of zFP538 [$(3-5.9) \times 10^{-5}$ M], the recovery of fluorescence was observed not only after acidification to pH ∼5.2 but even after acidification to pH ∼3. Thus, aggregation stabilizes the protein against acid denaturation, and this is maintained by complete recovery of absorbance and fluorescence of zFP538 at high concentrations after reverse titration from acidic to neutral conditions.

The data obtained to date do not allow us to propose an exact mechanism of the acidic denaturation of zFP538 but do enable us to make certain assumptions. Since the denaturation kinetics in the pH range from 3.75 to 4.24 is described with two exponents, there are at least three forms of the protein, two of which are fluorescent. From the data on continuous titration of the protein in the concentration range of $10^{-6}-10^{-9}$ M (Figure 5), it is possible to conclude that at least one irreversible transition exists (denaturation of the protein) because after a decrease in the concentration, neither fluorescence nor absorption (Figure 2B) is fully restored upon returning to neutral conditions. Since at a high protein concentration (3×10^{-5} M) the change in fluorescence is completely reversible in the continuous titration with acid, i.e., there is no irreversible denaturation (Figure 3), one may assume that disaggregation is a first concentration-dependent process after which denaturation of the protein becomes possible. The dimensions of the aggregates determine, in turn, the differences in denaturation kinetics at different concentrations. Thus, to explain the kinetics of acidic denaturation of zFP538, the following simplest scheme can be proposed:

$$zFP538_1 \Leftrightarrow zFP538_2 \rightarrow zFP538_3$$

where the first form is an aggregated protein, the second form is the protein with another degree of aggregation, and the third form is the denaturated protein.

The appearance of the third exponent in eq 1 at pH 3.5 can be explained by the additional transition between the spectral forms with fluorescence intensities at 540 and 580 nm ($zFP538_{580}$):

$$\begin{array}{c} zFP538_1 \Leftrightarrow zFP538_2 \rightarrow zFP538_3 \\ \Updownarrow \\ zFP538_{580} \end{array}$$

The appearance of the plateau on the kinetic curves at pH >4.24 indicates the existence of a "lag" period during which some transitions take place, but these transitions have little or no influence on fluorescence. This may be due to an accumulation of some intermediate form that causes an initiation of a gradual decrease of fluorescence only after the accumulation of this intermediate form at a sufficient concentration.

The fact that the aggregation of zFP538 is pH-dependent suggests an electrostatic nature of the aggregation. This agrees with previous results (*14*) in which the replacement of positively charged amino acid residues located near the N-terminus resulted in reduced aggregation.

The data obtained indicate that zFP538 in films exists in the form of fluorescing granules of ellipsoid form. The major and minor half-axels of the ellipses differ two to three times. Two independent methods (AFM and gel filtration) clearly show the existence of aggregates of about 5000−9000

monomers. It is interesting to note that color proteins in corals exist as fluorescent pigment granules (FPGs) 0.5−1.2 μm in diameter, which are packed into specialized cells or are present in the cytoplasm of various other nonspecialized cells (*30*). Since we have observed the formation of granules with similar dimensions in the films of zFP538, one may assume that the formation of fluorescent pigment granules in corals may be due to the intrinsic properties of GFP-like proteins.

Fluorescent pH titration of solutions of high concentration of zFP538 revealed transitions with p*K* near 4.5 and within the 5.95−6.30 region. As protein concentration decreased, additional transitions with p*K* within 3.41−3.85, 6.57−6.87, and 7.69−7.89 appeared (Table 1). It is interesting to note that transitions with p*K* values within 6.80−6.87 and 7.69−7.89 observed in diluted solutions of zFP538 practically coincide with p*K* of the isolated chromophore (*25*). The transitions observed in concentrated protein solutions have p*K* values noncharacteristic for chromopeptides of zFP538. These transitions apparently correspond to changes in protein conformation.

One of the possible explanations of the pH dependence of spectral properties of zFP538 upon aggregation may be as follows. The formation of high molecular weight aggregates leads to increased rigidity of the chromophore environment and prevents possible irreversible changes upon acidification. Due to increased rigidity in tight aggregates, the freedom of the chromophore mobility is restricted, causing a more intensive fluorescence (see below). Similar behavior is described for phycobiliproteins (PBs). The function of these proteins is to collect and to transmit quanta of light to the photosystem during photosynthesis. PBs in cyanobacteria and red algae are assembled into structurally complex supramolecular particles (with M_rs ranging from 5 million to 20 million), the phycobilisomes (*19*, *21*, *31*−*33*). Assemblies of higher molecular weights exhibit a more intensive fluorescence in comparison to that of small aggregates of PBs (*32*). The basic structural unit of phycobilisomes is the disk-shaped hexamers or trimers of PBs (*21*, *31*, *33*).

The changes in the absorption and fluorescence of PBs under aggregation or dissociation can be due to a number of reasons, such as the appearance of exciton splitting between close chromophores in the aggregates, change of interactions between the chromophores and their environment, and/or changes in the chromophore geometry, occurring upon dissociation (see below) (*17*, *18*, *20*, *34*, *35*).

Chromophores of phycobiliproteins are open-chain tetrapyrroles (bilins) connected by monocarbon linkages. The shape of bilin molecules can change from a fully opened linear form to a porphyrin-like pseudocyclic form. The former is characterized by the predominance of the visible band (500−700 nm) in the absorption spectrum as compared with UV band (300−400 nm), while the latter has an inverse ratio of visible and UV absorption maxima (*17*, *36*, *37*). X-ray structure analysis showed that the chromophores in the native phycobiliproteins exist mainly in the energetically less favorable stretched plane form, which is maintained by the noncovalent interactions with the amino acid chromophore environment (*38*). Protein denaturation results in the decrease of fluorescence quantum yield that correlates completely with the acquisition of a pseudocyclic form by the chromophores and is well tracked by the change in absorbance spectra (*17*). It was suggested that a change in the chromophore to a slightly more cyclic conformation, occurring as a result of the dissociation of oligomers into monomers, could lower its absorbance (*18*, *35*). Conversion of a pseudocyclic to a linear configuration is possible when free rotation of pyrroles of the chromophore around *exo*-cyclic single and double bonds can take place. It is this phenomenon that determines the almost total absence of fluorescence of the free bilin pigments in solution at room temperature caused by twisting around methene bridges. Twisting is a common and a rapid relaxation pathway for chromophores containing *exo*-cyclic double bonds (*39*). When bound to a protein, the chromophores are fixed more tightly, giving rise to the bright emission of the phycobiliproteins (*17*, *40*).

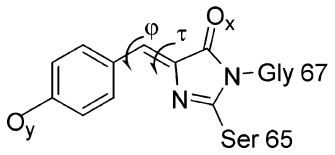

FIGURE 17: 4-(*p*-Hydroxybenzylidene)imidazolin-5-one (structure of the GFP chromophore). The O_y, O_x, and N atoms are possible protonation sites. The φ and τ dihedral angles can rotate in the excited state (*43*−*45*).

There is another possible way by which aggregation can influence spectral properties of PBs. When aggregates (or oligomers) are produced, a change in the structural support of each monomer occurs. In the high molecular weight aggregates, each protein is packed with another protein, unlike the situation of smaller oligomers and monomers, where water replaces the proteins. Thus, quenching of the phycobiliprotein's fluorescence by a solvent decreases, resulting in more intensive emission. For example, the various complexes of phycocyanin with the nonpigmented polypeptides in phycobilisomes exhibit a red-shifted and an increased absorbance and fluorescence spectral intensity. The phycocyanin−polypeptide complexes showed fluorescence emission intensities 2−3-fold higher than those of phycocyanin under the same conditions (*32*).

The three-dimensional structure of zFP538 is still unknown; however, it is most probable that it is a β-barrel typical of color proteins. The structure of the chromophore of color fluorescent proteins [4-(*p*-hydroxybenzylidene)-imidazolin-5-one with different substituents] (*26*, *41*, *42*) resembles the tetrapyrrole structures of chromophore prosthetic groups of phycobiliproteins since they both contain methene bridges between the aromatic rings. As was mentioned above, the presence of such bridges stipulates the existence of a certain nonradiative pathway for energy relaxation of the excited biliprotein molecules. A similar phenomenon is probably observed in the case of the zFP538 protein. Free rotation around *exo*-methylene double bond may occur in the yellow protein monomer and lead to a lower quantum yield of fluorescence. The possibility of such rotation is described for the GFP chromophore (rotation around φ and τ dihedral angles in the excited state is shown in Figure 17) (*43*−*45*). Inhibition of isomerization of the *exo*-methylene double bond is reported to explain the bright fluorescence of the chromophore within GFP as compared with the synthetic model compound of the chromophore and peptide fragment of GFP bearing the chromophore (*46*). The

fast internal conversion in mutants of GFP is due to freedom for torsional motions of the chromophore (*44*). The formation of high molecular weight aggregates promotes a rigid fixation of protein structure and decreased free rotation of zFP538 chromophore, resulting ultimately in brighter fluorescence. In addition to decreasing the vibrations and rotations of the chromophore in the excited state, the formation of high molecular weight aggregates may prevent the penetration of a solvent into protein molecules, thus decreasing the probability of fluorescence quenching upon contact with the solvent. These assumptions are based on the fact that the protein in concentrated solutions is highly aggregated and is more stable against fluorescence quenching on acidification unlike the less concentrated solutions where the protein according to the gel filtration data exists in the form of less molecular weight particles.

Phycobiliproteins carry out the function of regulating the "amount of light" ["light-harvesting" antennae of PBs (*21*, *31*, *33*)]. Fluorescent proteins may also have a similar photoregulatory function (*30*, *47*). To carry out their functions in cyanobacteria and red algae, PBs are self-organized into antenna-like high molecular weight complexes composed of trimers and hexamers, and this aggregation is pH-dependent. C-Phycocyanin, for example, is a hexamer at pH 5−6 and dissociates into trimers at pH 7 (*16*). Cryptomonad biliprotein phycocyanin 645 has a different pH-dependent equilibrium: fast and reversible dissociation of dimers into monomers takes place when the pH changes from 6 to 4 (*18*). In comparison with the mainly hexameric phycocyanins and phycoerythrins, allophycocyanin has a weaker tendency to aggregate and exists as a trimer in solution. Monomers of the allophycocyanin can be obtained by acidification of the solution up to pH 3.9 (*23*). Similar to PBs, GFP-like color fluorescent proteins exhibit a tendency to form aggregates; moreover, their chromophores show some similarities to PBs structure. On this basis it is also possible to draw some analogy between PBs and FPs in the correlation between the structure of the protein and its spectral properties. The similarity of nonradiative relaxation of GFP to linear tetrapyrroles and some structurally related aromatic compounds has been noted (*44*). We suggest that the pH-dependent aggregation property of FPs has profound similarities to the in vivo phycobilisome-like organization of high molecular weight complexes that carry out photoregulatory functions in nature.

ACKNOWLEDGMENT

We are grateful to Dr. G. McDermott, Berkeley National Laboratory, Berkeley, CA, for assistance in the experiments on dynamic light scattering, Dr. E. Dementieva for help in manuscript preparation, and Dr. Anya Salih for fruitful discussion of the manuscript.

REFERENCES

1. Ward, W. W., and Bokman, S. H. (1982) Reversible denaturation of *Aequorea* green-fluorescent protein: Physical separation and characterization of the renatured protein, *Biochemistry 21*, 4535−4540.
2. Ward, W. W. (1998) Biochemical and physical properties of green fluorescent protein, in *Green Fluorescent protein: properties, applications, and protocols* (Chalfie, M., and Kain, S., Eds.) pp 45−75, Wiley-Liss, New York.
3. Yang, F., Moss, L. G., and Phillips, G. N., Jr. (1996) The molecular structure of green fluorescent protein, *Nat. Biotechnol. 14*, 1246−1251.
4. Brejc, K., Sixma, T. K., Kitts, P. A., Kain, S. R., Tsien, R. Y., Ormö, M., and Remington, S. J. (1997) Structural basis for dual excitation and photoisomerization of the *Aequorea victoria* green fluorescent protein, *Proc. Natl. Acad. Sci. U.S.A. 94*, 2306−2311.
5. Zacharias, D. A., Violin, J. D., Newton, A. C., and Tsien, R. Y. (2002) Partitioning of lipid-modified monomeric GFPs into membrane microdomains of live cells, *Science 296*, 913−916.
6. Cubitt, A. B., Heim, R., Adams, S. R., Boyd, A. E., Gross, L. A., and Tsien, R. Y. (1995) Understanding, improving and using green fluorescent proteins, *Trends Biochem. Sci. 20*, 448−455.
7. Tsien, R. Y. (1998) The green fluorescent protein, *Annu. Rev. Biochem. 67*, 509−544.
8. Baird, G. S., Zacharias, D. A., and Tsien, R. Y. (2000) Biochemistry, mutagenesis, and oligomerization of DsRed, a red fluorescent protein from coral, *Proc. Natl. Acad. Sci. U.S.A. 97*, 11984−11989.
9. Jakobs, S., Subrumaniam, V., Schönle, A., Jovin, T. M., and Hell, S. W. (2000) EGFP and DsRed expressing cultures of *Escherichia coli* imaged by confocal, two-photon and fluorescence lifetime microscopy, *FEBS Lett. 479*, 131−135.
10. Wall, M. A., Socolich, M., and Ranganathan, R. (2000) The structural basis for red fluorescence in the tetrameric GFP homolog DsRed, *Nat. Struct. Biol. 7*, 1133−1138.
11. Yarbrough, D., Wachter, R. M., Kallio, K., Matz, M. V., and Remington, S. J. (2001) Refined crystal structure of DsRed, a red fluorescent protein from coral, at 2.0-Å resolution, *Proc. Natl. Acad. Sci. U.S.A. 98*, 462−467.
12. Cotlet, M., Hofkens, J., Habuchi, S., Dirix, G., Van Guyse, M., Michiels, J., Vanderleyden, J., and De Schryver, F. C. (2001) Identification of different emitting species in the red fluorescent protein DsRed by means of ensemble and single-molecule spectroscopy, *Proc. Natl. Acad. Sci. U.S.A. 98*, 14398−14403.
13. Campbell, R. E., Tour, O., Palmer, A. E., Steinbach, P. A., Baird, G. S., Zacharias, D. A., and Tsien, R. Y. (2002) A monomeric red fluorescent protein, *Proc. Natl. Acad. Sci. U.S.A. 99*, 7877−7882.
14. Yanushevich, Y. G., Staroverov, D. B., Savitsky, A. P., Fradkov, A. F., Gurskaya, N. G., Bulina, M. E., Lukyanov, K. A., and Lukyanov, S. A. (2002) A strategy for the generation of nonaggregating mutants of *Anthozoa* fluorescent proteins, *FEBS Lett. 511*, 11−14.
15. Matz, M. V., Fradkov, A. F., Labas, Y. A., Savitsky, A. P., Zaraisky, A. G., Markelov, M. L., and Lukyanov, S. A. (1999) Fluorescent proteins from nonbioluminescent Anthozoa species, *Nat. Biotechnol. 17*, 969−973.
16. Saito, T., Isono, N., and Mizuno, H. (1974) Solution properties of phycocyanin, *Bull. Chem. Soc. Jpn. 47*, 1375−1381.
17. Stadnichuk, I. N. (1990) Phycobiliproteins, *Biol. Chem. (Moscow) 40*, 1−196.
18. MacColl, R., Malak, H., Cipollo, J., Label, B., Ricci, G., MacColl, D., and Eisele, L. E. (1995) Studies on the dissociation of cryptomonad biliproteins, *J. Biol. Chem. 270*, 27555−27561.
19. Wilk, K. E., Harpor, S. J., Jankova, L., Edler, D., Keenan, G., Sharples, F., Hiller, R. G., and Curmi, P. M. (1999) Evolution of a light-harvesting protein by addition of new subunits and rearrangement of conserved elements: Crystal structure of a cryptophyte phycoerythrin at 1.63-Å resolution, *Proc. Natl. Acad. Sci. U.S.A. 96*, 8901−8906.
20. Liu, J.-Y., Jiang, T., Zhang, J.-P., and Liang, D.-C. (1999) Crystal structure of allophycocyanin from red algae *Porphyra yezoensis* at 2.2-Å resolution, *J. Biol. Chem. 274*, 16945−16952.
21. Yu, M.-H., Glazer, A. N., and Williams, R. C. (1981) Cyanobacterial phycobilisomes. Phycocyanin assembly in the rod substructures of *Anabaena variabilis* phycobilisomes, *J. Biol. Chem. 256*, 13130−13136.
22. Glazer, A. N., Fang, S., and Brown, D. M. (1973) Spectroscopic properties of C-phycocyanin and of its α and β subunits, *J. Biol. Chem. 248*, 5679−5685.
23. MacColl, R., Csatorday, K., Berns, D. S., and Traeger, E. (1980) Chromophore interaction in allophycocyanin, *Biochemistry 19*, 2817−2820.
24. Foguel, D., and Weber, G. (1995) Pressure-induced dissociation and denaturation of allophycocyanin at subzero temperatures, *J. Biol. Chem. 270*, 28759−28766.
25. Zubova, N. N., Rudenko, N. V., and Savitsky, A. P. (2003) Aggregation strongly influences the pH-profile of fluorescence

of the yellow fluorescent protein zFP538, in *Proceedings of SPIE Genetically Engineered and Optical Probes for Biomedical Applications 4967* (Savitsky, A. P., Barnhop, D. J., Raghavachari, R., and Achilefu, S. I., Eds.) pp 88−99, SPIE, Bellingham, WA.
26. Zimmer, M. (2002) Green fluorescent protein (GFP): Applications, structure, and related photophysical behavior, *Chem. Rev. 102*, 759−781.
27. Ugarova N. N., Savitsky A. P., and Berezin I. V. (1981) The protoporphyrin apoperoxidase complex as a horseradish peroxidase analog. A fluorimetric study of the heme pocket, *Biochim. Biophys. Acta 662*, 210−219.
28. Vrzheshch, P. V., Akovbian, N. A., Varfolomeyev, S. D., and Verkhusha, V. V. (2000) Denaturation and partial renaturation of a tightly tetramerized DsRed protein under mildly acidic conditions, *FEBS Lett. 487*, 203−208.
29. Kneen, M., Farinas, J., Li, Y., and Verkman, A. S. (1998) Green fluorescent protein as a noninvasive intracellular pH indicator, *Biophys. J. 74*, 1591−1599.
30. Salih, A., Hoegh-Guldberg, O., and Cox, G. (1998) Photoprotection of symbiotic dinoflagellates by fluorescent pigments in reef corals, in *Proceedings of the Australian Coral Reef Society 75th Anniversary Conference* (Greenwood, J. G., and Hall, N. J., Eds.) pp 217−230, School of Marine Science, The University of Queensland, Brisbane.
31. Glazer, A. N. (1985) Light harvesting by phycobilisomes, *Annu. Rev. Biophys. Chem. 14*, 47−77.
32. Lundell, D. J., Williams, R. C., and Glazer, A. N. (1981) Molecular architecture of a light-harvesting antenna. *In vitro* assembly of the rod substructures of *Synechococcus* 6301 phycobilisomes, *J. Biol. Chem. 256*, 3580−3592.
33. Stec, B., Troxler, R. F., and Teeter, M. M. (1999) Crystal structure of C-phycocyanin from *Cyanidium caldarium* provides a new perspective on phycobilisome assembly, *Biophys. J. 76*, 2912−2921.
34. Sugimoto, T., Kikushima, M., Saito, M., and Suzuki, H. (1984) Models for the change in chromophore structure of allophycocyanin corresponding to its observed reversible change in absorbance, *J. Phys. Soc. Jpn. 53*, 873−881.
35. Berns, D. S., and MacColl, R. (1989) Phycocyanin in physical−chemical studies, *Chem. Rev. 89*, 807−825.
36. Falk, H., and Müller, N. (1983) Force field calculations on linear polypyrrole systems, *Tetrahedron 39*, 1875−1885.
37. Blauer, G., and Wagnier, G. (1975) Conformation of bilirubin and biliverdin in their complexes with serum albumin, *J. Am. Chem. Soc. 97*, 1949−1954.
38. Schirmer, T., Bode, W., and Huber, R. (1987) Refined three-dimensional structures of two cyanobacterial C-phycocyanins at 2.1 and 2.5 Å resolution. A common principle of phycobilin-protein interaction, *J. Mol. Biol. 196*, 677−695.
39. Greene, B. I., Lamola, A. A., and Shank, C. V. (1981) Picosecond primary photoprocesses of bilirubin bound to human serum albumin, *Proc. Natl. Acad. Sci. U.S.A. 78*, 2008−2012.
40. Zickendraht-Wendelstadt, B., Friedrich, J., and Rüdiger, W. (1980) Spectral characterization on monomeric C-phycoerythrin from *Pseudanabaena* W 1173 and its α and *β* subunits: energy transfer in isolated subunits and C-phycoerythrin, *Photochem. Photobiol. 31*, 367−376.
41. Zagranichny, V. E., Rudenko, N. V., Gorokhovatsky, A. Yu., Zakharov, M. V., Shenkarev, Z. O., Balashova, T. A., and Arseniev, A. S. (2004) zFP538, a yellow fluorescent protein from coral, belongs to the DsRed subfamily of GFP-like proteins but possesses the unexpected site of fragmentation, *Biochemistry 43*, 4764−4772.
42. Gross, L. A., Baird, G. S., Hoffman, R. C., Baldridge, K. K., and Tsien, R. Y. (2000) The structure of the chromophore within DsRed, a red fluorescent protein from coral, *Proc. Natl. Acad. Sci. U.S.A. 97*, 11990−11995.
43. Kummer, A. D., Wiehler, J., Schüttrigkeit, T. A., Berger, B. W., Steipe, B., and Michel-Beyerle, M. E. (2002) Picosecond time-resolved fluorescence from blue-emitting chromophore variants Y66F and Y66H of the green fluorescent protein, *ChemBioChem 3*, 659−663.
44. Kummer, A. D., Kompa, C., Lossau, H., Pöllinger-Dammer, F., Michel-Beyerle, M. E., Silva, C. M., Bylina, E. J., Coleman, W. J., Yang, M. M., and Youvan, D. C. (1998) Dramatic reduction in fluorescence quantum yield in mutants of green fluorescent protein due to fast internal conversion, *Chem. Phys. 237*, 183−193.
45. Chen, M. C., Lambert, C. R., Urgitis, J. D., and Zimmer, M. (2001) Photoisomerization of green fluorescent protein and the dimensions of the chromophore cavity, *Chem. Phys. 270*, 157−164.
46. Niwa, H., Inouye, S., Hirano, T., Matsuno, T., Kojima, S., Kubota, M., Ohashi, M., and Tsuji, F. I. (1996) Chemical nature of the light emitter of the *Aequorea* green fluorescent protein, *Proc. Natl. Acad. Sci. U.S.A. 93*, 13617−13622.
47. Salih, A., Larkum, A., Cox, G., Kühl, M., and Hoegh-Guldberg, O. (2000) Fluorescent pigments in corals are photoprotective, *Nature 408*, 850−853.

BI048274C